

Synthesis and characterization of a mercury-containing trimetalloboride†

Cite this: *Chem. Commun.*, 2014, 50, 5729

Received 17th February 2014,
Accepted 8th April 2014

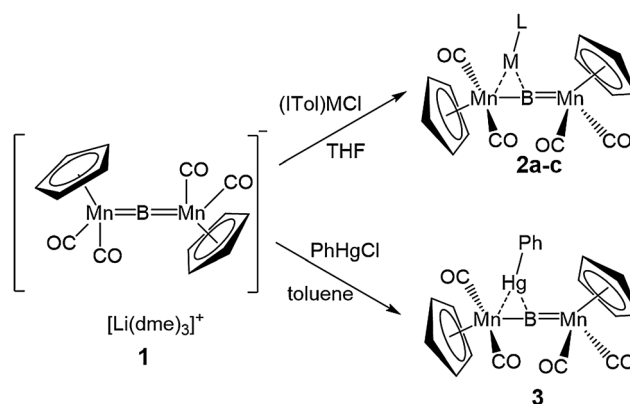
DOI: 10.1039/c4cc01246a

www.rsc.org/chemcomm

The reaction of phenylmercuric chloride with an anionic dimanganese borylene ($\text{Li}^+[\text{Cp}_2(\text{CO})_4\text{Mn}_2\text{B}]^-$) led to the formation of a trimetalloboride featuring the first reported bond between mercury and a non-cluster boron atom. Examination by ^{199}Hg NMR indicated ^{11}B – ^{199}Hg scalar coupling. Theoretical calculations indicated the nature of bonding to be σ -donation from a B–Mn π -orbital to Hg, in conjunction with weak $\text{Hg}_d \rightarrow \pi^*$ back-donation.

Save for one very recent report,¹ covalent interactions between mercury and boron have been limited to systems containing borane clusters. Early instances of Hg–B bonding featured the insertion of Hg into the open face of decaborane (*nido*- $\text{B}_{10}\text{H}_{14}$), bound either *via* tetrahapto-coordination to 4-boron atoms in the 1:1 complex $[\text{B}_{10}\text{H}_{12}\text{HgMe}]^-$ or sandwiched between the open faces of two decaborane molecules in the 2:1 species $[(\text{B}_{10}\text{H}_{12})_2\text{Hg}]^{2-}$.^{2,3} Structural assignments of these two compounds were proposed solely on the basis of NMR or IR data, without the aid of X-ray crystallography. A handful of crystal structures were subsequently reported describing the binding of Hg to boron vertices of borane or carborane clusters as *exopolyhedral* substituents on individual boron atoms,⁴ or as bridging moieties between two or more boron vertices.⁵

For some time, we have been interested in the addition of low-valent members of the late d-block to metal–borylene bonds. To date, work in this area has yielded a number of new compounds with interesting bonding motifs.⁶ The addition of base-stabilized group 11 metals across the central $\text{Mn}=\text{B}=\text{Mn}$ unit of anionic dimanganese borylene **1**⁷ has recently been shown to give addition products **2a–c** with the elimination of LiCl (Scheme 1).⁸ In compounds **2a** and **2b**, Au and Ag inserted asymmetrically across



Scheme 1 Syntheses of trimetalloborides **2** and **3**. **2a**, M = Au; **2b**, M = Ag; **2c**, M = Cu. ITol = *N,N'*-bis(4-methylphenyl)imidazol-2-ylidene.

one of the two B=Mn bonds, elongating the proximate borylene bond with respect to the unaffected bond on the opposite side of the molecule. In **2c**, Cu occupied a symmetric position equidistant from each Mn, forming Mn–B–Cu angles near 90°. Computational investigation indicated diffuse delocalized bonding between Au, B and the proximate Mn in **2a**, while in **2c** the interaction of $(\text{ITol})\text{Cu}^+$ and the borylene anion was primarily electrostatic.

The isoelectronic nature of the closed-shell $\text{d}^{10}\text{-Au}^+$ and -Hg^{2+} cations, as well as their shared relativistic behavior and propensity toward the formation of linear 14-electron species,⁹ suggested the reactivity of Hg^{2+} complexes with **1** similar to the addition of $[(\text{ITol})\text{Au}]^+$ in the formation of **2a**. When **1** was treated with PhHgCl in toluene, the emergence of a bright red color was accompanied by the precipitation of a colorless solid. Examination of the reaction mixture by ^{11}B NMR indicated the growth of a low-field resonance at 208 ppm, coincident with the disappearance of a peak at 199 ppm characteristic of **1**. After filtration and concentration of the filtrate, the product (**3**) was crystallized at -35°C . Though stable at -35°C , slow decomposition of **3** was evident at room temperature.

The solid-state structure of **3**, determined by single crystal X-ray crystallography (Fig. 1), bears a striking resemblance to **2a**.

^a Institut für Anorganische Chemie, Julius-Maximilians-Universität Würzburg, Am Hubland, 97074 Würzburg, Germany. E-mail: h.braunschweig@uni-wuerzburg.de

^b Tezpur University, Napaam 784028, Assam, India

^c University of Sussex, Brighton BN1 9QJ, Sussex, UK

† Electronic supplementary information (ESI) available: Full experimental and spectroscopic description of the work described herein, as well as relevant computational details and Fig. S1–S5. CCDC 975393. For ESI and crystallographic data in CIF or other electronic format see DOI: 10.1039/c4cc01246a

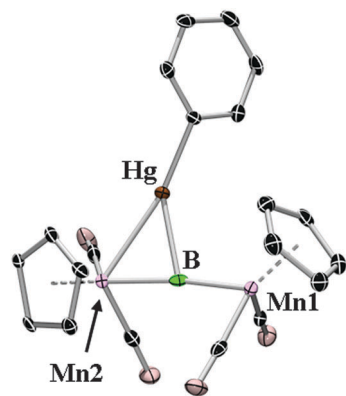


Fig. 1 The crystallographically determined structure of one of the two independent molecules of **3**. Thermal ellipsoids represent 50% probability. Hydrogen atoms have been omitted for clarity. Selected bond lengths (Å) and bond angles (°) averaged for the 2 independent molecules: B–Hg, 2.2915; B–Mn1, 1.860; B–Mn2, 1.9555; Hg–Mn2, 2.655; Hg–C_{phenyl}, 2.089; Mn2–B–Hg, 76.9; Mn2–Hg–C_{phenyl}, 165.3; Mn2–B–Mn1, 173.5; Mn1–B–Hg, 109.2.

The Hg atom resides between B and Mn2 (Hg–B, 2.2915 Å; Hg–Mn2, 2.655 Å; (avg.)). Whereas the Mn–B–Mn unit in **1** is symmetric, with B–Mn bonds measuring 1.8812(14) Å and 1.8809(14) Å,⁷ the addition of mercury substantially elongates the B–Mn2 bond (1.9555 Å (avg.)), while inducing a slight contraction of the B–Mn1 bond (1.860 Å (avg.)). The Mn–B–Mn angle is nearly linear both before and after addition (**1**, 176.11(9)°; **3**, 173.5° (avg.)), while the Mn2–Hg–C_{phenyl} angle is slightly bent toward boron (165.27° (avg.)), reminiscent of the Mn–Au–C angle in **2a** (160.29(7)°), indicating a more complicated bonding environment than a pure σ -interaction between Mn and Hg.

The ¹H and ¹³C{¹H} NMR spectra of **3** in solution each show only one set of signals for the Cp-moiety at 4.17 ppm (¹H) and 82.6 ppm (¹³C). Furthermore, the ¹³C{¹H} NMR spectrum shows only one signal for the four CO groups (226 ppm), suggesting fluxional behavior in solution. Low-temperature ¹H NMR failed to induce separation of the Cp-resonances at temperatures as low as –90 °C. Spectroscopic inquiry at a faster time-scale (FT-IR) demonstrated the asymmetry of the ground state structure through excellent agreement between the room temperature solution-state FT-IR spectrum of **3** and a DFT-simulated IR spectrum based on an optimized structure of C₁-symmetry, closely resembling the solid-state structure of **3** (Fig. S1, ESI†).

Covalent bonding between Hg and B was confirmed by ¹⁹⁹Hg NMR spectroscopy. Fig. 2 compares the ¹¹B-coupled (Fig. 2a) and ¹¹B-decoupled (Fig. 2b) ¹⁹⁹Hg{¹H} spectra of **3**. The broad, slightly structured peak located at 83.9 ppm (FWHH = 460 Hz, Fig. 2a) was observed to substantially narrow with application of ¹¹B decoupling (FWHH = 33 Hz, Fig. 2b). The existence of well resolved ¹⁹⁹Hg satellites in the 500 MHz ¹H NMR spectrum of the *ortho*- and *meta*-protons (FWHH \approx 7 Hz) of the PhHg moiety indicated that relaxation *via* chemical shift anisotropy (CSA) was negligible for the ¹⁹⁹Hg nucleus in solution. A line-width comparison of the ¹⁹⁹Hg{¹H} NMR signal at 53.8 MHz (300 MHz NMR spectrometer) and the signal at 89.6 MHz (500 MHz NMR spectrometer) showed no difference, indicating that the observed line-width of the ¹⁹⁹Hg{¹H} resonance (460 Hz)

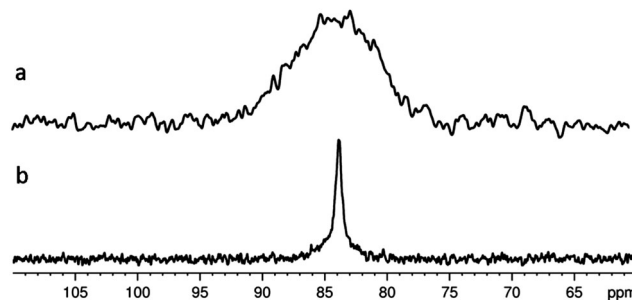


Fig. 2 (a) ¹⁹⁹Hg{¹H} NMR spectrum of **3**; (b) ¹⁹⁹Hg{¹H, ¹¹B} NMR spectrum of **3**. Both spectra were recorded on a 300 MHz Bruker Avance III HD NMR spectrometer.

arises from a combination of scalar coupling due to the neighboring boron (¹⁰B and ¹¹B) and motional narrowing due to fluxionality in solution. As scalar coupling (*J*) is indicative of covalent interactions between nuclei,¹⁰ the narrowing upon decoupling confirms the existence of bonding interactions between B and Hg. A ¹¹B-coupled ¹⁹⁹Hg NMR spectrum obtained at higher sensitivity (500 MHz) gave better resolution, showing a rough quartet of sufficient detail to allow the determination of *J*_{Hg–B} (103 Hz) through fitting of a simulated spectrum (Fig. S2, ESI†).

To examine the role mercury plays in the bonding of **3**, we performed theoretical calculations at the OLYP/TZP, QZ4P level of density functional theory using the ADF program.^{11–13} The optimized geometry is in good agreement with the observed structure (Fig. S3, ESI†). The asymmetric interaction of [PhHg]⁺ with the [(CpMn(CO)₂)₂B][–] fragment replicates the observed difference in Mn–B bond lengths (Mn2–B, 1.930 Å; Mn1–B, 1.824 Å). The Mayer Bond Order (MBO) of the shorter of the two Mn–B bonds is more than double that of the longer (Mn2–B, 0.566; Mn1–B, 1.168), further indicating diminished bonding between Mn2–B relative to Mn1–B. The MBO values obtained for the Hg–Mn2 (0.373) and Hg–B (0.471) bonds suggest both interactions to be weaker than true single bonds. A very weak interaction was observed between the distant Mn1 and Hg, with a MBO value of 0.134. Though this interaction is insignificant in the solid state, it may enable facile conversion between the two enantiomeric forms of **3** *via* transfer of the [HgPh]⁺ between the two B–Mn bonds in solution, explaining the fluxionality observed by ¹H NMR spectroscopy.

Extended Transition State-Natural Orbitals for Chemical Valence (ETS-NOCV)¹⁴ calculations are useful tools for the identification and quantification of orbital interactions involved in the bonding between molecular fragments.¹⁵ The two pairs of complementary NOCV determined to be relevant for bonding between the [PhHg]⁺ and [Mn–B–Mn][–] fragments are a σ -interaction of a π -orbital between Mn2 and B with [PhHg]⁺ (Fig. 3a) and back-donation from a mercury d-orbital to an orbital of π^* -symmetry between B and Mn2 (Fig. 3b). The deformation densities ($\Delta\rho$) depict the stabilization attributed to each interaction, quantified by their respective ΔE values (σ , –73.7 kcal mol^{–1}; π , –5.7 kcal mol^{–1}), indicating that the primary contributor to bonding is the σ -interaction. The transferred charge in this interaction, indicated by $\Delta\rho_1$, is evenly spread across both Mn and B, explaining both

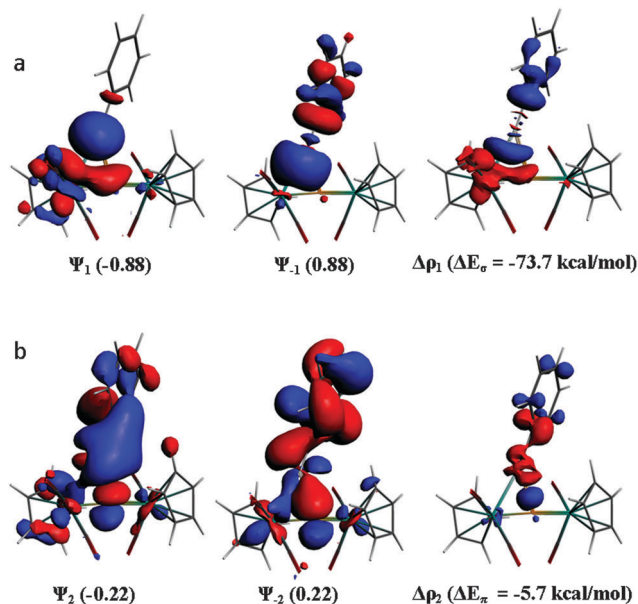


Fig. 3 Plots of relevant bonding NOCV pairs (Ψ_n/Ψ_{-n}) with accompanying eigenvalues, the associated deformation densities ($\Delta\rho_n$) and the orbital stabilization energies (ΔE) corresponding to (a) σ -donation and (b) π -back donation. Positive and negative eigenvalues correspond to bonding and antibonding interactions, respectively. The direction of charge flow in the deformation densities is from red \rightarrow blue.

the non-linearity of the Mn2–Hg–C_{phenyl} angle and the comparatively small value of $J_{\text{Hg-B}}$ measured by ^{199}Hg NMR.¹⁶ This bonding arrangement is similar to analysis of **2a**, describing a diffuse interaction between B, Mn, and Au,^{8a} and analysis of **3** by QTAIM (Fig. S4, ESI†) showed a bond path between B and Hg curved toward Mn2, indicative of delocalized bonding.^{8a} ETS-NOCV analysis of model compound **2a**_{Ime} ([Cp₂(CO)₄Mn₂]B–Au(Ime), Ime = *N,N'*-dimethylimidazol-2-ylidene) showed a comparable σ -interaction between [(Ime)Au]⁺ and [Mn–B–Mn][–] (Fig. S5a, ESI†).

The d \rightarrow π^* back-donation depicted in Fig. 3b represents a much smaller energetic influence; however, its existence is notable. Despite its residence in the d-block of the periodic table, mercury has traditionally been considered a “post-transition metal”.^{9,17} Dicationic Hg²⁺ is thought to be unable to participate in the types of orbital interactions common to its lighter neighbors due to its d¹⁰ closed-shell configuration and presumed lack of d-orbital participation in bonding, though a few studies have cast doubt on this classification. The synthesis of a d⁹ Hg(III)-containing species was reported as early as 1976,¹⁸ but the validity of this assignment has subsequently been called into question.¹⁹ The prediction of the gas-phase stability of d⁸-square planar HgF₄ (ref. 20) was followed by its detection in a frozen neon matrix.²¹ In 2010, Gabbai reported the transition-metal behavior of an Hg²⁺ ion tethered in close proximity to a Lewis acidic Sb-center,²² though XANES data for the same system would later indicate negligible participation of the Hg d-orbitals in the bonding interaction.²³ Previous computational work has hinted the possibility of very weak back-donation from filled d-orbitals on Hg to π -accepting moieties.²⁴

If this back-donation is present in **3**, it should be even more prevalent in the geometrically-similar **2a**, since Au⁺ is both in a

lower oxidation state and is thought to more readily employ its d-orbitals in bonding.²⁵ The classification of Au⁺ as a transition metal is not in question,⁹ and recent analysis has attributed significant strength to Au_d \rightarrow π^* interactions with alkenes.²⁶ ETS-NOCV analysis of **2a**_{Ime} (Fig. S5b, ESI†) indicates very similar d \rightarrow π^* back-donation to that seen in the analysis of **3**. As expected, the back-donation in the model compound **2a**_{Ime} ($\Delta E_\pi = 15.1 \text{ kcal mol}^{-1}$) is stronger than in **3**, comprising $\sim 23\%$ of the combined bonding interactions, whereas the Hg_d \rightarrow π^* back-donation is only $\sim 7\%$ of the calculated total.

The similarities between the back-donation interactions of an accepted transition metal (Au) and a “controversial” transition metal (Hg) placed in the same system suggest the capability of Hg to function akin to its neighbors to its left, though the small magnitude of the interaction indicates a reluctance to do so in this system. Ongoing work on engineering related bonding environments with this capability in mind will no doubt provide further experimental evidence for, or against, the transition-metal-nature of Hg.

Financial support in the form of an advanced grant from the European Research Council is gratefully acknowledged.

Notes and references

- 1 A. V. Protchenko, D. Dange, A. D. Schwartz, C. Y. Tang, N. Philips, P. Mountford, C. Jones and S. Aldridge, *Chem. Commun.*, 2014, **50**, 3841.
- 2 (a) N. N. Greenwood and N. F. Travers, *Chem. Commun.*, 1967, 216; (b) N. N. Greenwood and D. N. Sharrocks, *J. Chem. Soc. A*, 1969, 2334.
- 3 (a) N. N. Greenwood, B. S. Thomas and D. W. Waite, *J. Chem. Soc., Dalton Trans.*, 1975, 299; (b) N. N. Greenwood, *Pure Appl. Chem.*, 1977, **49**, 791.
- 4 (a) V. I. Bregadze, V. TS. Kampel and N. N. Godovikov, *J. Organomet. Chem.*, 1976, **112**, 249; (b) V. I. Bregadze, *Chem. Rev.*, 1992, **92**, 209; (c) Z. Zheng, M. Diaz, C. B. Knobler and M. F. Hawthorne, *J. Am. Chem. Soc.*, 1995, **117**, 12338; (d) Z. Zheng, C. B. Knobler, C. E. Curtis and M. F. Hawthorne, *Inorg. Chem.*, 1995, **34**, 432; (e) M. F. Hawthorne and Z. Zheng, *Acc. Chem. Res.*, 1997, **30**, 267; (f) I. A. Lobanova, V. I. Bregadze, S. V. Timofeev, P. V. Petrovskii, Z. A. Starikova and F. M. Dolgushin, *J. Organomet. Chem.*, 2000, **597**, 48; (g) V. I. Bregadze, I. A. Lobanova, S. V. Timofeev, A. R. Kudinov, V. I. Meshcheryakov, O. L. Tok, P. V. Petrovskii and Z. A. Starikova, *J. Organomet. Chem.*, 2002, **657**, 171; (h) Z. A. Starikova, I. A. Lobanova, S. V. Timofeev and V. I. Bregadze, *J. Mol. Struct.*, 2009, **937**, 61.
- 5 (a) C. P. Magee, L. G. Sneddon, D. C. Beer and R. N. Grimes, *J. Organomet. Chem.*, 1975, **86**, 159; (b) N. A. Hosmane and R. N. Grimes, *Inorg. Chem.*, 1979, **18**, 2886; (c) D. C. Finster and R. N. Grimes, *Inorg. Chem.*, 1981, **20**, 863; (d) J. Yang, C. Zheng, J. A. Maguire and N. S. Hosmane, *Inorg. Chem. Commun.*, 2004, **7**, 111; (e) F. Texidor, J. A. Ayllón, C. Viñas, R. Kivekäs, R. Sillanpää and J. Casabó, *J. Organomet. Chem.*, 1994, **483**, 153; (f) K. F. Shaw, B. D. Reid and A. J. Welch, *J. Organomet. Chem.*, 1994, **482**, 207; (g) T. Schaper and W. Preetz, *Z. Naturforsch., B: Chem. Sci.*, 1997, **52**, 57.
- 6 (a) H. Braunschweig, D. Rais and K. Uttinger, *Angew. Chem., Int. Ed.*, 2005, **34**, 3763; (b) H. Braunschweig, C. Burschka, M. Buzler, S. Metz and K. Radacki, *Angew. Chem., Int. Ed.*, 2006, **45**, 4352; (c) H. Braunschweig, K. Radacki, D. Rais and K. Uttinger, *Organometallics*, 2006, **25**, 5159; (d) H. Braunschweig, K. Radacki, D. Rais and F. Seeler, *Angew. Chem., Int. Ed.*, 2006, **45**, 1066; (e) H. Braunschweig, M. Buzler, T. Kupfer, K. Radacki and F. Seeler, *Angew. Chem., Int. Ed.*, 2007, **46**, 7785; (f) H. Braunschweig, M. Buzler, R. D. Dewhurst, K. Radacki and F. Seeler, *Z. Anorg. Allg. Chem.*, 2008, **634**, 1875.
- 7 H. Braunschweig, M. Buzler, R. D. Dewhurst and K. Radacki, *Angew. Chem., Int. Ed.*, 2008, **47**, 5650.
- 8 (a) H. Braunschweig, P. Brenner, R. D. Dewhurst, M. Kaupp, R. Müller and S. Östreicher, *Angew. Chem., Int. Ed.*, 2009, **48**, 9735; (b) H. Braunschweig, A. Damme, R. D. Dewhurst, T. Kramer,

- S. Östreicher, K. Radacki and A. Vargas, *J. Am. Chem. Soc.*, 2013, **135**, 2313.
- 9 F. A. Cotton, G. Wilkinson, C. A. Murillo and M. Bochmann, *Advanced Inorganic Chemistry*, Wiley, New York, 6th edn, 1999.
- 10 M. H. Levitt, *Spin Dynamics: Basics of Nuclear Magnetic Resonance*, Wiley, New York, 2002.
- 11 ADF2013.01; SCM, Theoretical Chemistry, Vrije Universiteit: Amsterdam, The Netherlands; <http://www.scm.com>.
- 12 The TZP basis set was used for the main group elements and the QZ4P basis set was used for the Mn and Hg atoms. Dispersion corrections were incorporated using Grimme's DFT-D3-BJDAMP term. S. Grimme, S. Ehrlich and L. Goerigk, *J. Comput. Chem.*, 2011, **32**, 1456.
- 13 (a) R. F. Nalewajski, J. Mrozek and A. Michalak, *Int. J. Quantum Chem.*, 1997, **61**, 589; (b) A. Michalak, R. L. De Kock and T. J. Ziegler, *J. Phys. Chem. A*, 2008, **112**, 7256.
- 14 (a) M. Mitoraj and A. Michalak, *J. Mol. Model.*, 2007, **13**, 347; (b) A. Michalak, M. Mitoraj and T. Ziegler, *J. Phys. Chem. A*, 2008, **112**, 1933.
- 15 For some recent examples see: (a) M. Mitoraj and A. Michalak, *Organometallics*, 2007, **26**, 6576; (b) M. P. Mitoraj and A. Michalak, *Inorg. Chem.*, 2011, **50**, 2168; (c) Z. D. Brown, P. Vasko, J. C. Fetting, H. M. Tuononen and P. P. Power, *J. Am. Chem. Soc.*, 2012, **134**, 4045; (d) A. Manikkamäki, P. P. Power and H. M. Tuononen, *Organometallics*, 2013, **32**, 6690; (e) I. Seidu, M. Seth and T. Ziegler, *Inorg. Chem.*, 2013, **52**, 8378; (f) C. Werle, C. Bailly, L. Karmazin-Brelot, X.-F. Le Góff, L. Ricard and J.-P. Djukic, *J. Am. Chem. Soc.*, 2013, **135**, 17839; (g) S. Ndambuki and T. Ziegler, *Inorg. Chem.*, 2013, **52**, 3860.
- 16 Known examples of scalar coupling between boron and mercury have substantially larger $J_{\text{Hg-B}}$ values, ranging from ~ 1000 – 3000 Hz. For example see ref. 4c and d.
- 17 N. N. Greenwood and A. Earnshaw, *Chemistry of the Elements*, Pergamon, Oxford, 1984.
- 18 R. L. Deming, A. L. Allred, A. R. Dahl, A. W. Herlinger and M. O. Kestner, *J. Am. Chem. Soc.*, 1976, **98**, 4132.
- 19 S. Riedel, M. Straka and M. Kaupp, *Chem. – Eur. J.*, 2005, **11**, 2743.
- 20 (a) M. Kaupp and H. G. von Schnering, *Angew. Chem., Int. Ed. Engl.*, 1993, **32**, 861; (b) M. Kaupp, M. Dolg, H. Stoll and H. G. von Schnering, *Inorg. Chem.*, 1994, **33**, 2122.
- 21 X. Wang, L. Andrews, S. Riedel and M. Kaupp, *Angew. Chem., Int. Ed.*, 2007, **46**, 8371.
- 22 T.-P. Lin, C. R. Wade, L. M. Pérez and F. P. Gabbaï, *Angew. Chem., Int. Ed.*, 2010, **49**, 6357.
- 23 T.-P. Lin, R. C. Nelson, T. Wu, J. T. Miller and F. P. Gabbaï, *Chem. Sci.*, 2012, **3**, 1128.
- 24 W. Petz, B. Neumüller, S. Klein and G. Frenking, *Organometallics*, 2011, **30**, 3330.
- 25 (a) H.-C. Tai, I. Krossing, M. Seth and D. V. Deubel, *Organometallics*, 2004, **23**, 2343; (b) I.-S. Ke and F. P. Gabbaï, *Inorg. Chem.*, 2013, **52**, 7145.
- 26 (a) N. Salvi, L. Belpassi and F. Tarantelli, *Chem. – Eur. J.*, 2010, **16**, 7231; (b) D. Zuccaccia, L. Belpassi, A. Macchioni and F. Tarantelli, *Eur. J. Inorg. Chem.*, 2013, 4121; (c) G. Bistoni, L. Belpassi and F. Tarantelli, *Angew. Chem., Int. Ed.*, 2013, **52**, 11599.